






Mechanical and Thermal Properties of Self-Curing Metakaolin-based Geopolymer Mortar in Hot-arid Climate



Keltoum Bekraoui^{*} , Hamid Khelafi^{2,3} , Mohamed Mouli¹ , Mhammed Abdeldjalil^{2,3} 
and Aida Bensekhria⁴ 

¹Laboratoire des Matériaux LABMAT, 31000, National Polytechnic School of Oran Maurice Audin, Oran, Algeria

²Civil Engineering Department, (UADA) University African Ahmed Draïa, 01000 Adrar, Algeria

³Laboratory of LMST USTO Oran, Algeria

⁴LRNAT Laboratory, Geology Department, Batna 2 University A, Batna, Algeria

Abstract:

Aims: This work evaluates the potential of locally obtained moderate-grade kaolinitic clay from Tabelbala, Algeria, for manufacturing metakaolin-based geopolymer mortar with improved mechanical and thermal properties in hot-arid conditions.

Background: Urban heat islands and environmental concerns related to cement production drive the search for sustainable alternatives. Geopolymer binders can substitute for Portland cement with lower carbon emissions and better thermal performance. The low reactivity of local materials like Tabelbala clay requires enhancement.

Objective: This study aimed to optimize the geopolymerization process by enhancing the reactivity of Tabelbala clay by using silica fume and alkaline activators. Additionally, it evaluated the impact of curing conditions on its mechanical and thermal properties.

Method: Kaolinitic clay was calcined at 900 °C to produce metakaolin, and the activation was performed using sodium hydroxide, potassium hydroxide, and silica fume or sodium silicate solution. Using ambient and solar curing techniques, geopolymer mortars were analyzed for their compressive and flexural strengths, shrinkage, bulk density, porosity, and thermal conductivity.

Result: Solar curing significantly enhanced compressive strength (up to 37.4 MPa) and flexural strength (up to 12 MPa) at 28 days. Adding silica fume also reduced drying shrinkage and thermal conductivity with a marked improvement in density.

Conclusion: Even though the Tabelbala clay is of moderate quality when combined with silica fume and cured optimally, it can produce geopolymer mortars with excellent mechanical and thermal properties, demonstrating their suitability as sustainable construction materials for arid climates.

Keywords: Metakaolin-based geopolymer, Alkali activators, Solar curing, Mechanical strength, Thermal conductivity, Arid zone.

© 2025 The Author(s). Published by Bentham Open.

This is an open access article distributed under the terms of the Creative Commons Attribution 4.0 International Public License (CC-BY 4.0), a copy of which is available at: <https://creativecommons.org/licenses/by/4.0/legalcode>. This license permits unrestricted use, distribution, and reproduction in any medium, provided the original author and source are credited.

* Address correspondence to this author at the Laboratoire des Matériaux LABMAT, 31000, National Polytechnic School of Oran Maurice Audin, Oran, Algeria; E-mail: keltoum.bekraoui@enp-oran.dz

Cite as: Bekraoui K, Khelafi H, Mouli M, Abdeldjalil M, Bensekhria A. Mechanical and Thermal Properties of Self-Curing Metakaolin-based Geopolymer Mortar in Hot-arid Climate. Open Civ Eng J, 2025; 19: e18741495381331. <http://dx.doi.org/10.2174/0118741495381331250213070615>



Received: January 04, 2025
Revised: January 18, 2025
Accepted: January 29, 2025
Published: March 18, 2025



Send Orders for Reprints to
reprints@benthamscience.net

1. INTRODUCTION

With arid zones currently covering more than 30% of the Earth's land surface and supporting over a third of the global population, sustainable construction materials in these areas are more urgent than ever [1, 2]. The expected growth of these regions due to climate change further underscores this need. Over the past century, significant urban centres have emerged in dry areas worldwide, such as cities in Iran and Syria [3]. These cities face complex challenges, such as the effects of urban heat islands. According to several studies, Urban Heat Islands (UHIs) can often raise urban air temperatures by 2 to 15 °C. The Urban area centres in arid and semi-arid countries might see 2 to 4 °C temperature increases relative to their rural environs [4, 5]. This phenomenon increases water use and energy consumption by increasing air conditioning and pollution demand. This effect, in turn, has consequences for public health and quality of life [6].

Carbon dioxide emissions from cement manufacture exacerbate the urban heat island effect and accelerate global warming rates. It is estimated to be the global source of 4-7% of total carbon dioxide emissions. Manufacturing one ton of cement generates 900 kg of carbon dioxide into the atmosphere [7, 8].

In addition, a large portion of the urban heat island effect is attributable to using heat-trapping building materials such as cementitious concrete and asphalt. Therefore, it is imperative to choose construction materials carefully to offset the impact of heat islands since dense, dark-coloured materials retain sunlight for an extended period and then re-emit this heat to the urban air at night [9].

An extensive literature study suggests that geopolymer cement is a viable and sustainable substitute for

conventional Portland cement in the building sector, primarily because its carbon dioxide emissions during manufacturing are six times lower than those of Portland cement [10].

The creation of geopolymer cement involves using aluminosilicate materials, which can originate from geological sources such as kaolinite, metakaolin, and red mud or from industrial and agricultural by-products like blast furnace slag, silica fume, waste glass, fly ash, and rice husk ash. These materials are combined with alkali activators, including potassium hydroxide (KOH), sodium hydroxide (NaOH), sodium silicate (Na_2SiO_3), and potassium silicate (K_2SiO_3). Geopolymer Concrete (GPC) typically demonstrates enhanced mechanical and durability properties compared to Ordinary Portland Cement (OPC) concrete [11].

Furthermore, geopolymer concrete made from metakaolin possesses a unique set of advantageous characteristics. It is porous, lightweight, fire-resistant, and moisture-proof. Additionally, it can absorb and release water vapour, making it superior to traditional insulating materials. These properties make passive cooling of buildings in hot, arid regions particularly intriguing, as they do not adhere to the same insulation regulations as those applicable in cold areas [12, 13].

The construction field in arid zones is also adversely affected by high temperatures during the summer, which significantly affects the final quality of concrete. It causes the need for significant and costly precautions during the realization of works (using admixtures) and delays in the completion of construction [14]. Meanwhile, the requirement for heat curing is one significant factor in Geopolymer fabrication, which restricts its application to cast in situ industry [15].



Fig. (1). Location of Tabelbala within Algeria kaolin deposit + kaolin and metakaolin powder Coordinates: 29°24'N 3°15'W.

Table 1. Physic-chemical properties of starting materials %.

Chemical Composition (wt. %)											
Oxide	SiO ₂	Al ₂ O ₃	Fe ₂ O ₃	CaO	MgO	SO ₃	K ₂ O	Na ₂ O	TiO ₂	P ₂ O ₅	LOI
Kaolin	52.65	26.17	1.061	0.51	0.11	1.01	1.88	0.41	1.53	0.12	10.35
Metakaolin	56.69	32.15	2.77	0.48	0.34	0.32	2.1	-	1.5	0.132	
Silica fume	94.57	1	1	0.4	1	-	1.6	-	-	-	-
OPC	19.71	4.77	3.14	57.59	3.41	2.53	0.83		-	-	2.53
Physical properties											
Blaine specific surface (m ² /kg)						3400					
BET-specific surface m ² /g						14.6718					

At ambient temperatures, geopolymer concrete tends to develop low strength early, whereas higher temperatures significantly enhance strength over ambient temperature curing [16]. So much work has been done to avoid this problem. Singh *et al.* [17] indicated that fly ash could be partially replaced with slag to prevent curing heat. Bharat Jindal [18] demonstrated that ambient cured geopolymer concrete is a feasible alternative to traditional Portland cement-based concrete, offering significant mechanical and durability properties without the need for elevated temperature curing.

Several works have reported that the addition of nanoparticles such as nano-silica, nano-alumina, nano-calcium carbonate, and nano-clay improves the geopolymerization process at room temperature and exhibits appreciable enhancement in structural behaviour at different ages without any heat activation [19, 20]. Thus, the nanoparticles reduced sorptivity and increased the compressive strength of the mixes.

W. Hu *et al.* [21] proposed heating techniques for cast-in-place geopolymer piles. Laboratory and field tests demonstrated that the applied heating methods significantly enhanced the strength development of the piles, allowing them to reach the required resistance faster and with lower energy consumption. In contrast, the control pile, which lacked a heating system, exhibited inferior strength characteristics. Therefore, the geopolymer pile with heating systems could be a promising and energy-efficient solution.

Previous literature mainly focused on enhancing geopolymer performance with minimal emphasis on the effect of self-curing conditions on mechanical strength and thermal conductivity [22-26]. Despite research on self-curing, geopolymer formation relied solely on room ambient curing. For example, Sayed *et al.* [27] examined the impact of combining multiple alkali activators at varying concentrations and the incorporation of nanoparticles on the workability of geopolymer.

Recent research has focused on enhancing the durability of geopolymers in hot, dry areas. For example, El Dandachy *et al.* [28] studied how high temperatures affect geopolymer mortars made from metakaolin. They showed that these mortars retain good compressive strength and low thermal conductivity, making them suitable for these climates. Another study by Ahmed *et al.*

[29] investigated using bricks made from industrial waste. The aim was to improve building design to make homes more energy-efficient in desert areas. The results showed improved thermal insulation and energy savings compared with conventional materials.

Research by Emdadi *et al.* [30] demonstrated that integrating geopolymers into passive cooling devices could significantly lower internal construction temperatures in arid zones. In addition, Khater and Gawaad [31] highlighted the impact of nanomaterials on optimizing the thermal and mechanical characteristics of geopolymer mortars, focusing particularly on their use in environments subject to significant temperature variations.

There have been limited studies on the combined influence of the arid area climate and the geopolymerization mechanism on the thermal performance of geopolymers. In this study, we conduct a comprehensive investigation into the mechanical and thermal properties of geopolymer mortar derived from moderate kaolin sourced from Tabalbala, located in the arid southwest region of Algeria.

The research focuses on optimizing critical mixing parameters, including the concentrations of NaOH and KOH, the alkaline activator solution-to-binder ratio, and the liquid-to-solid mass ratio, as these factors play a pivotal role in determining the physical and mechanical performance of the resulting geopolymer. Additionally, the study examines the influence of these parameters on early shrinkage and thermal conductivity. Particular attention is given to the combined effects of different types of activators and curing conditions, both at ambient room temperature and under solar-induced heating, on key properties such as compressive strength, bulk density, porosity, and thermal conductivity.

2. MATERIALS AND METHODS

2.1. Dry Ingredients

This study utilized moderate-grade kaolin clay, sourced from Tabelbala in southern Algeria, as the primary aluminosilicate material for producing metakaolin-based geopolymer mortars (Fig. 1). The kaolin clay was processed by crushing it with a jaw crusher, followed by grinding it using a disk mill, and then sieving it to achieve a particle size of less than 20 µm. The resulting powder

was calcined in a muffle furnace at 900 °C for durations of 1, 2, 3, and 4 hours, with a controlled heating rate of 10 °C per minute, to convert the kaolin into metakaolin (MK). The optimal thermal activation conditions for the kaolin were identified by evaluating the strength activity index (SAI %) [32].

The raw and calcined clay samples were analyzed by X-ray fluorescence, Fourier Transform Infrared (FTIR) spectra, and X-Ray Diffraction (XRD) analysis to determine the chemical and mineralogical compositions. Then, physical characteristics such as BET-specific surfaces were defined. We added Commercial Silica Fume (SF), obtained from GRANITEX (Algeria region) with a specific surface $>15 \text{ m}^2/\text{gr}$ and a high percentage of amorphous silica ($\text{SiO}_2 = 94.57\%$), to the geopolymer mixtures to enhance the geopolymerization process.

The reference sample mortars were prepared using Ordinary Portland Cement (OPC) type CEMII /A-p 42.5 N from STG SIDI MOUSSA Adrar. Mortar specimens were prepared using DIN-EN 196-1 standard sand (S) with a high percentage silica content of 98% as fine aggregate. Table 1 presents the chemical composition of the starting materials, metakaolin and silica fume, as determined by an X-Ray Fluorescence (XRF) spectrometer.

2.2. Alkaline Activators

The main ingredients in the alkaline activator solutions were sodium hydroxide (NaOH), potassium hydroxide (KOH), and liquid sodium silicate (Na_2SiO_3). We purchased

all these ingredients from Sigma Aldrich. The NaOH powder has 99% purity with a 2.13 g/cm^3 density, and the KOH pellets have 85% purity with a 2.04 g/cm^3 density. At the same time, the sodium silicate solution contains 10.6% SiO_2 and 26.5% Na_2O with a density of 1.39 g/cm^3 and a pH of 11.30. We prepared the NaOH and KOH solutions with 19 M and 13.389 M molarities and cooled them at room temperature (Fig. 2).

Four distinct activator solutions were prepared by combining NaOH and KOH solutions with liquid sodium silicate or silica fume. These solutions were left to rest at room temperature for 24 hours to allow the formation of soluble silicate species. The prepared activator solutions were mixed with metakaolin and standard sand and mechanically stirred until a homogeneous mixture was achieved. The resulting mixtures were poured into $40 \times 40 \times 160 \text{ mm}$ moulds for compressive and flexural strength testing. The moulds containing the resulting mixtures were vibrated for 2 minutes before curing to minimize air entrapment.

2.3. Mix Proportions

Table 2 presents the proportions of each ingredient used in the formulation of 10 different geopolymer mix types, where the quantity of one ingredient was varied in each mix. Each mix was repeated thrice to ensure accuracy, resulting in 60 mixes. The samples were then subjected to two different curing methods: ambient and solar drying.



Fig. (2). The preparation of alkaline activators and metakaolin geopolymer mortars and curing regime.

Table 2. Mix proportions of OPC and MK geopolymer mortars.

Geopolymer Sample	Activators	Liquid/solid Mass Ratio	Cement	Metakaolin/wt	Silica Fume/wt	NaOH Solution		KOH Solution		Sodium Silicate	Sand	Added Water (g)
						g	Molarity	g	Molarity			
TE	/	0.5	450	/	/	/	/	/	/	/	1350	225
TS	/	0.5	450	/	/	/	/	/	/	/	1350	225
M1E/M1S	NaOH	0.5	/	320	100	161	19	/	/	/	1350	165
M ² E/M ² S	NaOH	0.4	/	320	100	161	19	/	/	/	1350	115
M3EM3S	NaOH	0.3	/	320	100	161	19	/	/	/	1350	66
M4E/M4S	KOH	0.5	/	320	100	/	/	225	13.389	/	1350	139
M5E/M5S	KOH	0.4	/	320	100	/	/	225	13.389	/	1350	90
M6E/M6S	KOH	0.3	/	320	100	/	/	225	13.389	/	1350	40
M7E/M7S	NaOH + Na ₂ SiO ₃	0.55	/	340	/	83	19	/	/	314	1350	35
M8E/M8S	NaOH + Na ₂ SiO ₃	0.5	/	340	/	83	19	/	/	314	1350	/
M9E/M9S	KOH + Na ₂ SiO ₃	0.55	/	329	/	/	/	115	13.389	302	1350	25
M10E/M10S	KOH + Na ₂ SiO ₃	0.5	/	329	//	/	/	115	13.389	302	1350	/

Table 3. Mix oxide molar ratios of alkaline activators and curing condition.

Geopolymer Sample	Activators	Liquid /Binder	SiO ₂ /Al ₂ O ₃ Molar Ratio	M ₂ O/SiO ₂ Molar Ratio	M ₂ O/Al ₂ O ₃ Molar Ratio	H ₂ O/M ₂ O Molar Ratio	Curing Condition
M1E ^a /M1S ^b	NaOH	0.5	3.6	0.28	1	13.5	Ambient/Solar
M ² E/M ² S	NaOH	0.4	3.6	0.28	1	10.8	Ambient/Solar
M3EM3S	NaOH	0.3	3.6	0.28	1	8.1	Ambient/Solar
M4E/M4S	KOH	0.5	3.6	0.28	1	13.9	Ambient/Solar
M5E/M5S	KOH	0.4	3.6	0.28	1	11.2	Ambient/Solar
M6E/M6S	KOH	0.3	3.6	0.28	1	8.44	Ambient/Solar
M7E/M7S	NaOH + Na ₂ SiO ₃	0.55	3.3	0.3	1	14.4	Ambient/Solar
M8E/M8S	NaOH + Na ₂ SiO ₃	0.5	3.3	0.3	1	12.6	Ambient/Solar
M9E/M9S	KOH + Na ₂ SiO ₃	0.55	3.3	0.3	1	14.7	Ambient/Solar
M10E/M10S	KOH + Na ₂ SiO ₃	0.5	3.3	0.3	1	13.35	Ambient/Solar

Note: a: E refers to the specimens that have undergone ambient curing.

b: S refers to the specimens that have undergone solar curing.

The calculations accounted for the total moles of silica provided by the metakaolin and silica fume. Similarly, we determined the water content by considering the contributions from all sources within the alkaline activators, including the hydroxide, potassium, and sodium silicate solutions, and added water. This experiment proposes replacing the sodium silicate solution with silica fume, using 49% silica fume by the total weight of the binder. All geopolymer mortars were prepared with a binder-to-sand ratio of 1:2.75. The liquid-to-binder ratio varied between 0.3 and 0.55. The SiO₂/M₂O ratio of 1 was selected to optimize gel formation while avoiding excessive alkali content that could negatively impact durability [33]. Varying the molar ratios SiO₂/Al₂O₃ (3.3–3.6), M₂O/SiO₂ (0.28–0.3) and H₂O/Na₂O (8.1–14.7) were investigated (Table 3).

The samples were prepared for comparison using a mixture of different materials, with the reference cement

mortar being prepared according to the specifications outlined in EN 196-1 [34]. The reference cement mortar contains 1350 g of standardized sand, 450 g of cement, and 225 g of water. This mixture served as the baseline for comparison with other samples, which were prepared using different methods to test the properties of the mortar and the resulting reactions.

2.4. Curing Condition

The eco-friendly treatment of mortars was selected to minimize costs and offer an environmentally sustainable alternative. In this context, we opted to utilize the abundant solar energy in hot regions to achieve this objective. The samples were divided into two groups: One of the parts of samples was stored at the same ambient temperature (E), while the other was placed outside to achieve sun resistance conditions (S). Solar curing was conducted outdoors with temperatures ranging from 35°C to 45°C, as measured using a calibrated thermometer.

Samples were exposed to direct sunlight daily for 28 days. The temperature and solar radiation recorded during the experimental period are presented in Fig. (3).

3. EXPERIMENTAL

3.1. Compressive and Flexural Strengths

The mechanical property tests of specimens, cured at 3, 14, and 28 days, were conducted following the procedures outlined in EN 196-1 [29] for MK-based geopolymer mortar and OPC reference mortars. The flexural strength of the mortar (40 mm × 40 mm × 160 mm) prisms was measured using the three-point bending test method by standard testing protocols. In contrast, the compressive strength of the mortar was determined by subjecting the specimen to a uniaxial load in a compression testing machine, ensuring accurate measurements of load-bearing capacity. Each test was conducted at least three times. For each experimental condition, a total of 20 geopolymer mixes were prepared. These included variations in curing temperature (ambient and solar). Each condition was repeated in triplicate to ensure reproducibility and statistical validity.

3.2. Drying Shrinkage and Bulk Density Test Method

Thirty-two different geopolymer mortar mixtures (M1, M4, M7, and M9) were prepared to study drying shrinkage (8 mixes), thermal conductivity (8 mixes), bulk density, and porosity (8 mixes). The variation in curing conditions (ambient and solar) was ensured within the experimental

design, with an appropriate number of samples allocated for each curing condition to guarantee the accuracy and reproducibility of the results.

The drying shrinkage test was conducted according to French standard NF P 15-433 [35] using a length comparator with a dial gauge accuracy of 0.0001 inch. Three mortar specimens (40 × 40 × 160 cm) were produced for each type, OPC and MK-based geopolymer, with a water-binder ratio of 0.5 Fig. (4).

After the test pieces were moulded, they were cured under standard conditions (20 ± 1°C and relative humidity, RH 90%) for 1 d, and then the mould was removed. Then, one part was conserved in the laboratory room under environmental temperature conditions, and the other was placed outside to achieve solar cure conditions.

The bulk density and porosity of the prism specimens were evaluated following ASTM C642-97 [36]. The specimens were heated at 105°C for 24 hours, cooled, and weighed (Wd). After soaking in water for 48 hours, the saturated surface dry weight (Wi) was measured. The specimens were then boiled for 5 hours and cooled, and the saturated surface dry weight (Wb) was recorded. The apparent weight in water (Ws) was obtained by suspending the specimen.

We measured thermal characterization tests on specimens of dimensions 100×100×50 mm³ in the ENPOran laboratory using the ISOMET 2104 equipment.

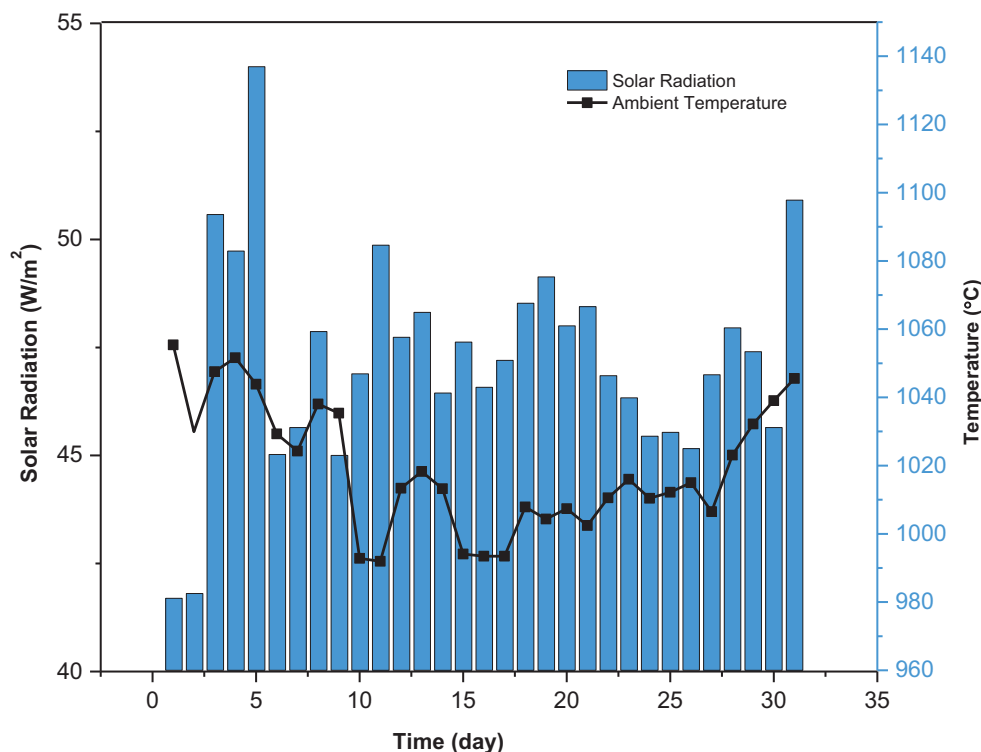


Fig. (3). The temperature and solar radiation recorded during the experimental period.

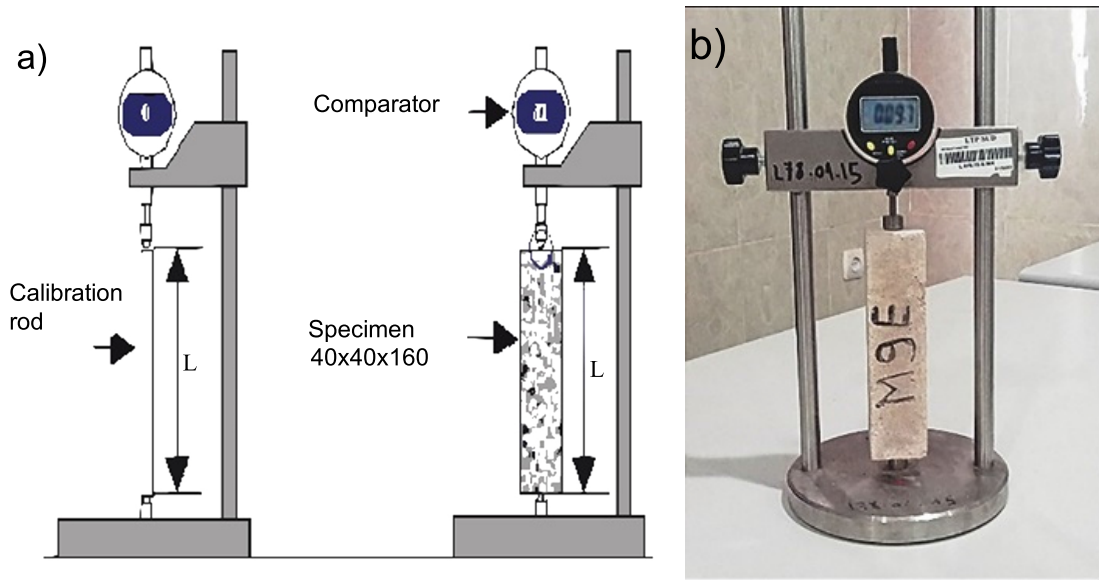


Fig. (4). Drying shrinkage measurements: (a) Shrinkage measurement method. (b) Strain measurements.

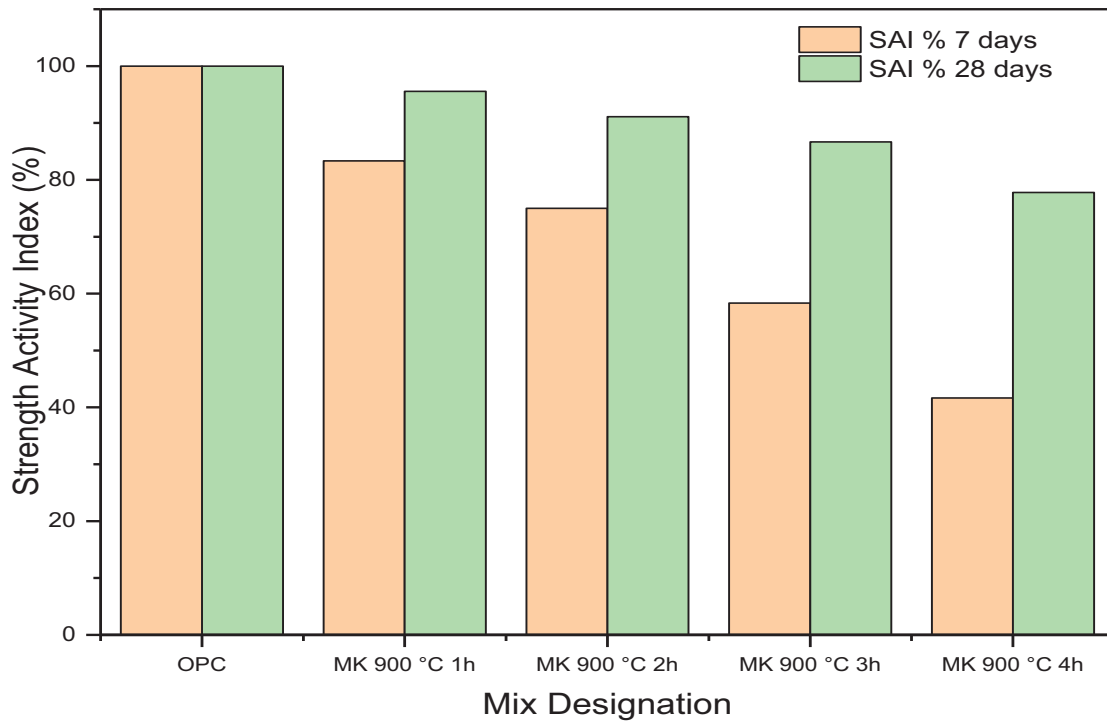


Fig. (5). Strength activity index of the mixes.

Additionally, residual fragments from the mortar compression tests were ground and sieved to a particle size < 45 μm. These samples were dried at 60°C for 24 hours before being subjected to X-ray diffraction analyses (XRD).

4. RESULTS

4.1. Metakaolin Activation

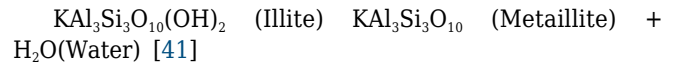
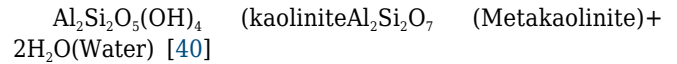
Thermal activation is widely recognized as a critical process for enhancing the reactivity of kaolin clay. The

findings presented in Fig. (5) indicate that the optimal conditions for achieving the highest strength activity index occur at a calcination temperature of 900 °C for one hour.

During the calcination of raw clay, the hydroxyl groups (OH)₂ are removed as water (H₂O), transforming the crystalline structure into an amorphous material and enhancing its reactivity [37, 38]. During the calcination of raw clay, the hydroxyl groups (OH)₂ are removed as water (H₂O), transforming the crystalline structure into an amorphous material and enhancing its reactivity [37, 38]. Infrared spectroscopy (FTIR) confirmed the dehydroxylation of kaolin clay, indicated by the removal of the stretching (-oh) bands at 3617-3696 cm⁻¹, as shown in Fig. (6a). The chemical composition of the treated kaolin aligns with astm c-618 standards for natural pozzolanic materials, supporting its application in concrete [39].

The high-temperature calcination weakens kaolinite's diffraction peaks and enhances quartz's diffraction peaks (Fig. 6b). Based on the analysis of the crystallinity of the raw and calcined samples by Origin software, it was found that the crystallinity of kaolin clay before calcination is 56.38% and that after calcination for 1h is 21.77%. Due to the moderate purity of the Tabalbala deposit, the obtained metakaolin contained about 27.87% of impurities, mainly quartz (18.9%), and the remaining 72% comprised

metakaolinite and metacillite as shown in Fig. (7).



The above results allowed us to determine the amount of amorphous silica and aluminium in the calcined clay. The geopolymer formulation will include SiO₂=38% and Al₂O₃=32%.

4.2. Compression and Flexure Strengths

The compressive strength results for geopolymer and Portland cement mortars at 3, 14, and 28 days are shown in Fig. (7). Most geopolymer samples displayed significantly lower early compressive strength (3 days) than the control specimens (TE and TS). Example: M3E (12.8 MPa, ambient) and M3S (14.3 MPa, solar) are much weaker than TE and TS at 3 days. The early strength of geopolymer materials is indeed influenced by slower geopolymerization, which relies on the alkaline activation of aluminosilicate precursors. This process typically results in lower initial strength than the rapid hydration of Ordinary Portland Cement (OPC), which forms calcium silicate hydrate (C-S-H) and provides higher initial strength [42, 43].

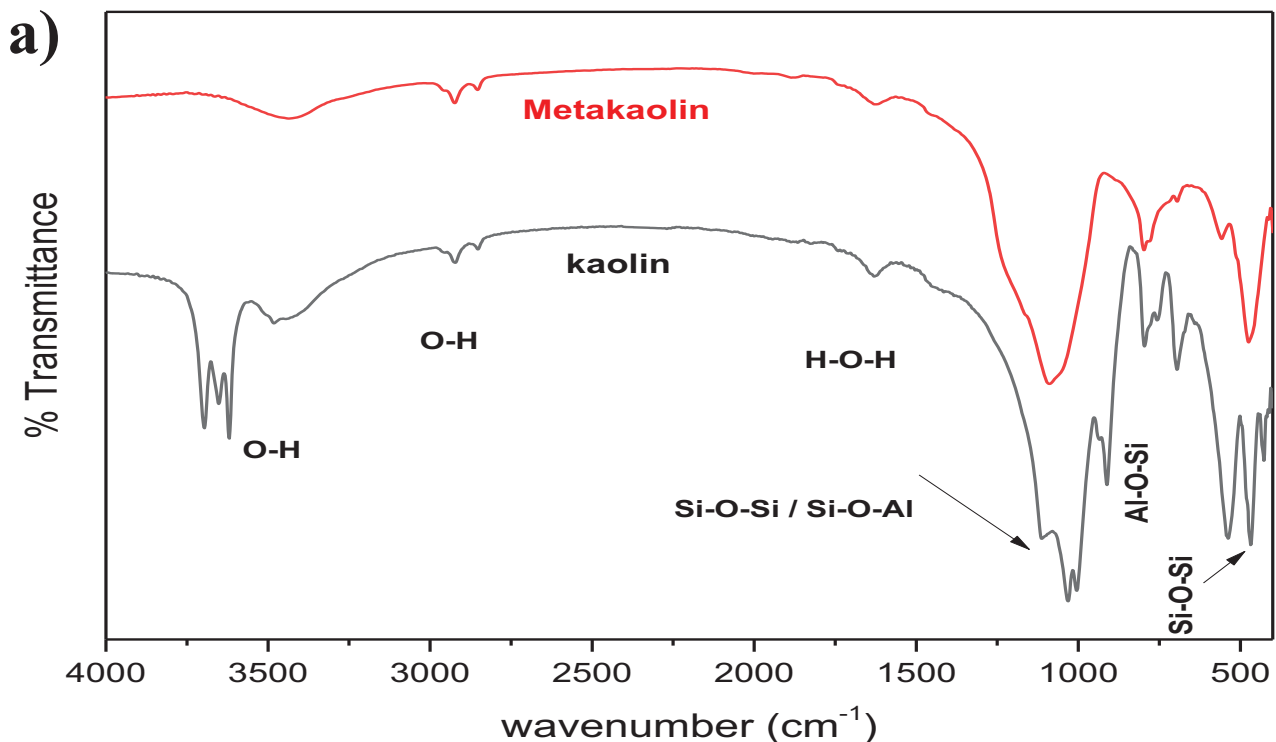


Fig. 8 contd.....

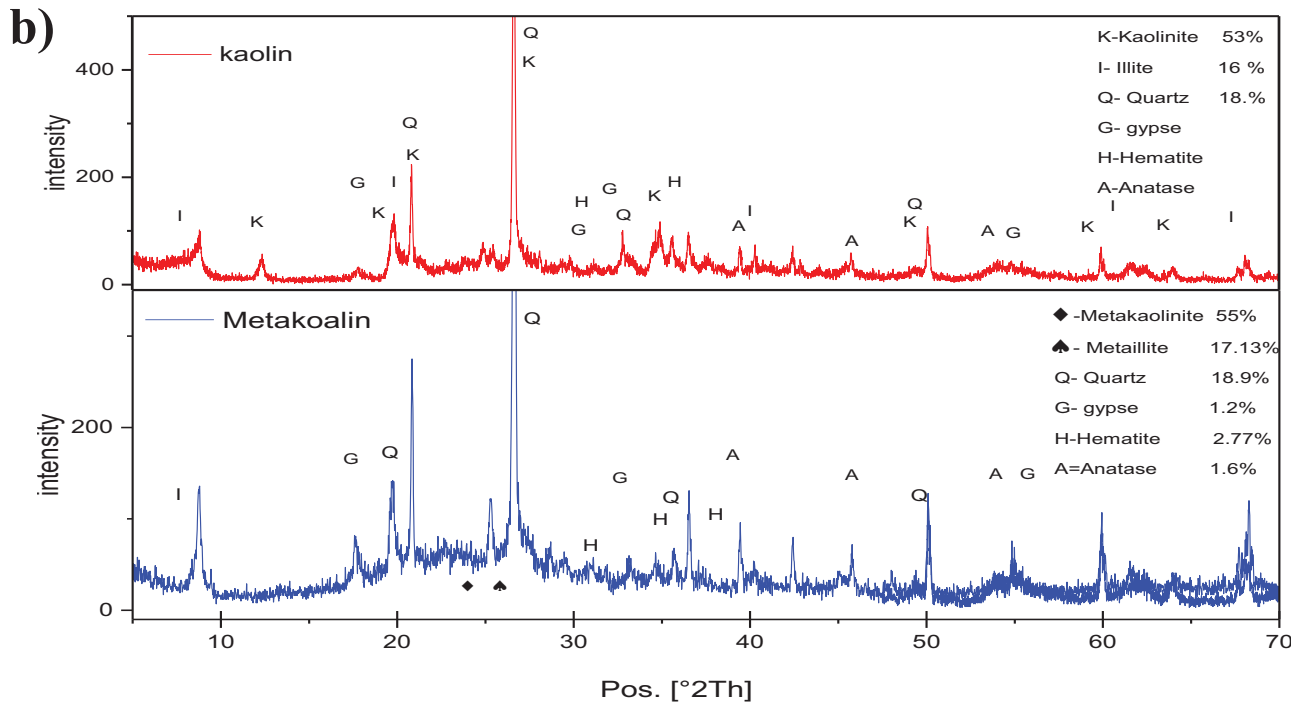


Fig. (6). a) FT-IR spectra and b) X-ray diffractograms of kaolin clay and metakaolin calcined at 900°C for 1 h.

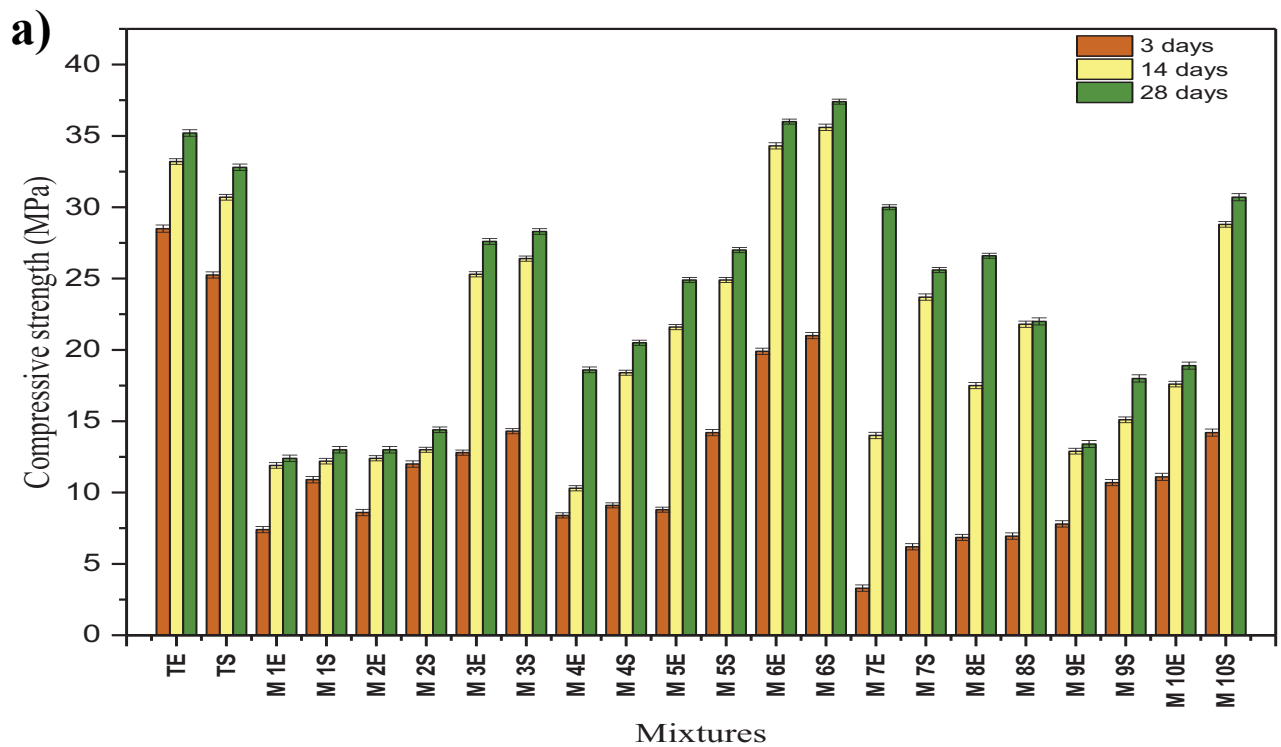


Fig. 9 contd.....

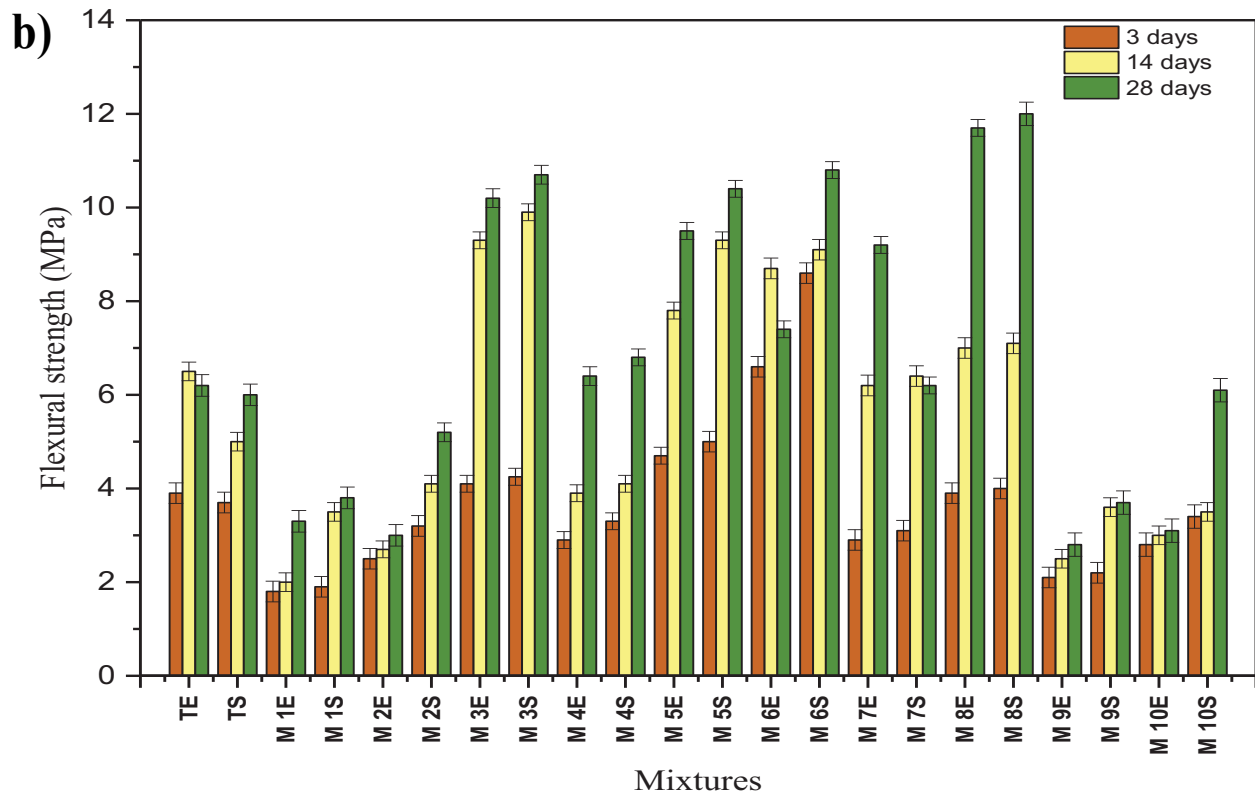


Fig. (7). a). Compressive and b). flexural strengths of GP and OPC mortars were measured at 3, 14, and 28 days under ambient and solar curing conditions.

In terms of strength at 14 and 28 days, solar curing significantly enhances geopolymer strength, often surpassing TS. Example: M6S achieves 35.6 MPa at 14 days and 37.4 MPa at 28 days, outperforming TS (30.7 MPa and 32.8 MPa, respectively). Ambient-cured geopolymers like M6E (34.3 MPa at 14 days, 36 MPa at 28 days) also approach or exceed TE's compressive strength.

Ambient-cured geopolymers showed strength enhancement over time. A similar trend was observed in solar-cured samples, whose long-term compressive strength may equal or exceed that of ambient-cured OPC mortars. This strength gain is associated with the continuous geopolymerization process, which contributes to improvements over time [11, 44].

As shown in Fig. (7), the early strength (3 days) of TE and TS outperforms most geopolymer samples in early flexural strength. For example, M3E (4.1 MPa) and M3S (4.25 MPa) are among the few geopolymer samples to meet or exceed TE's flexural strength at 3 days. In terms of strength at 14 and 28 days, solar-cured geopolymers often surpass TS in flexural strength at later ages. For example, M6S reaches 8.6 MPa at 14 days and 10.8 MPa at 28 days, well above TS. Ambient-cured samples like M6E also exhibit superior flexural strength (7.4 MPa at 28 days) compared to TE (6.2 MPa).

4.3. Effect of using NaOH or KOH as an Alkaline Activator

Silica fume combined with KOH results in higher strength due to the larger ionic radius of K^+ compared to Na^+ , forming a more stable aluminosilicate gel enriched with reactive silica [45]. As a result, network formation is enhanced, and the geopolymer matrix becomes denser, leading to improved compressive and flexural strength. While the sodium silicate solution already contains a high proportion of reactive silicates, the larger K^+ ions can delay condensation and lower compressive strength during early curing stages due to reduced aluminosilicate dissolution. This results in a less compact geopolymer network. Na^+ interacts more effectively with the sodium silicate, enhancing the dissolution and polymerization processes and leading to better strength development than KOH [46].

4.4. Effect of Curing Conditions on Compressive and Flexural Strengths

The effect of curing conditions on the compressive and flexural strengths of GP mortars is also evaluated in this study and is shown in Fig. (8a and 8b). The results demonstrated that solar curing accelerates geopolymerization reactions, leading to significantly higher compressive and flexural strength values at all ages (3, 14, and 28 days) than ambient curing.

Fig. (8a-d) demonstrates that solar curing enhances

compressive strength by approximately 3-5% while increasing flexural strength by 10-25%, primarily due to the elevated temperatures provided by sunlight. These higher temperatures increase the solubility and reaction rates of silica and alumina in the source material, which are crucial for forming the geopolymer gel (e.g., sodium

aluminosilicate hydrate (N-A-S-H), potassium aluminosilicate hydrate (K-A-S-H), or calcium aluminosilicate hydrate (C-A-S-H)). Furthermore, the elevated temperatures create conditions that facilitate faster condensation of the dissolved precursors, resulting in a denser and stronger geopolymer matrix [47].

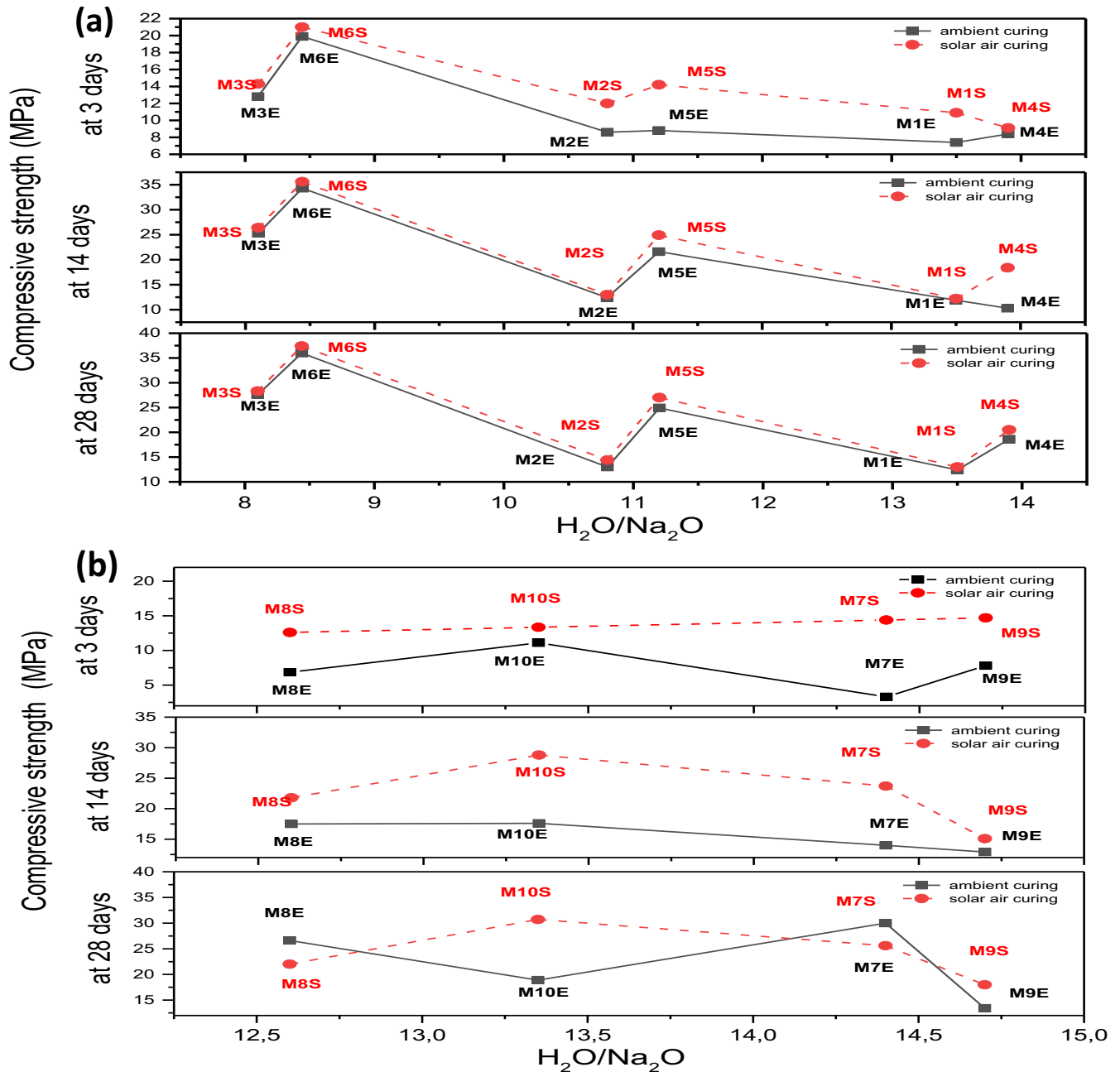


Fig. : contd....

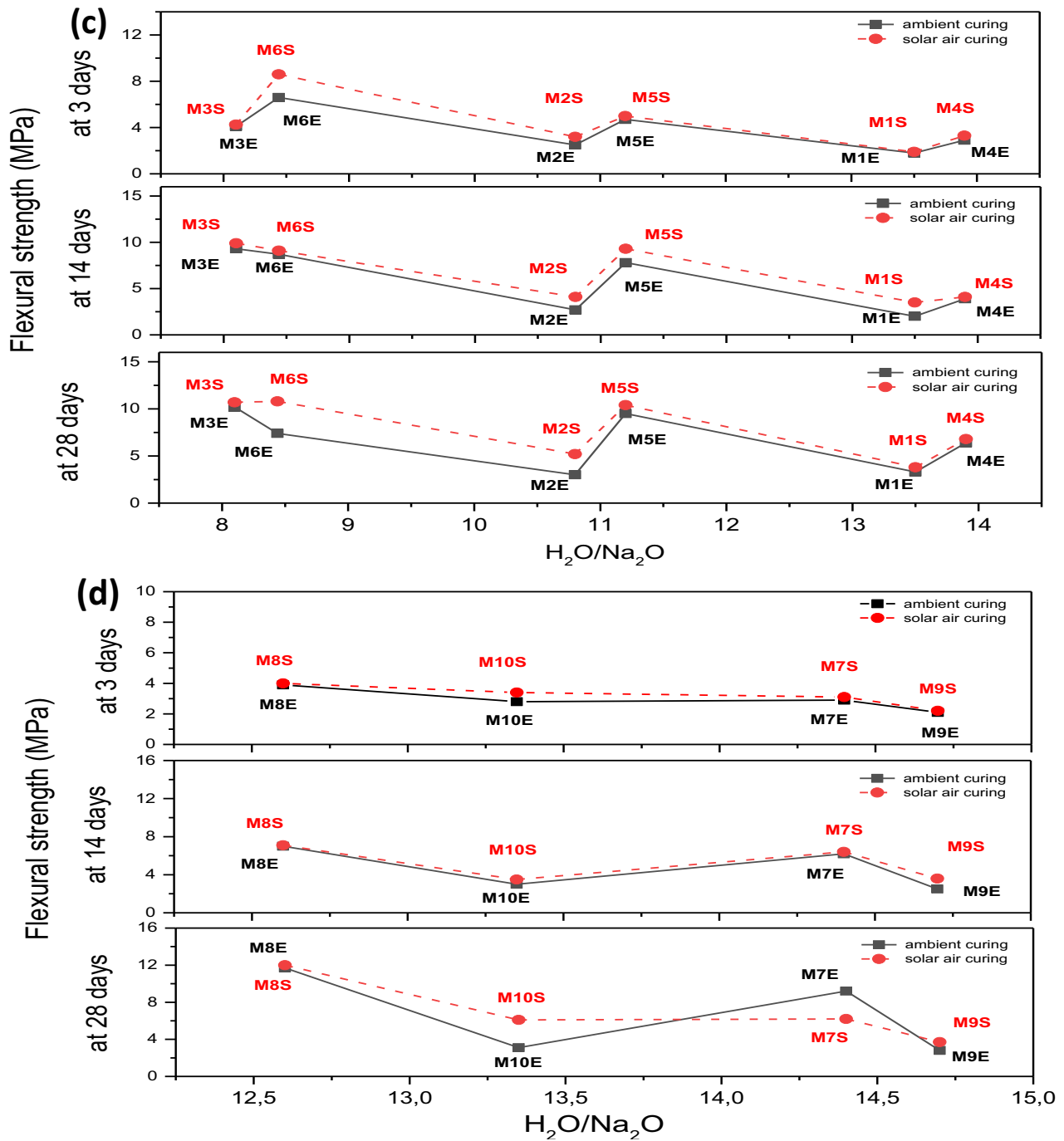


Fig. (8). Compressive and Flexural strengths of Geopolymer and OPC mortars 3, 14, and 28 days, with different H_2O/M_2O molar ratios. [a/c: SF+NH or KH, $SiO_2/Al_2O_3 = 3.6$, $Na_2O/SiO_2=0.28$ and $Na_2O//Al_2O_3 = 1$] & [b/d: SS+NH or KH, $SiO_2/Al_2O_3 = 3.3$, $Na_2O/SiO_2=0.3$ and $Na_2O//Al_2O_3 = 1$].

4.5. Effect of H_2O/M_2O Ratios

Compressive strength often diminishes when H_2O/M_2O ratios increase, as elevated water content develops a porous structure during drying. Fig. (8a, b) 1 demonstrate that samples with lower ratios (e.g., 8.1 or 8.44) consistently achieve higher compressive strengths (e.g.,

up to 37.4 MPa under solar curing).

In contrast, elevated ratios (e.g., 13.5 or 14.4) achieve weaker geopolymers, evidenced by decreased strengths over the same curing periods. (Fig. 8c, d) demonstrate that reduced H_2O/M_2O ratios (e.g., 8.1) provide increased flexural strengths attributable to the denser and more

cohesive gel network. Conversely, elevated ratios result in decreased flexural strength due to increased porosity. Compressive and flexural strengths often diminish when H_2O/M_2O ratios increase, as elevated water content develops a porous structure during drying. In contrast, elevated ratios achieve weaker geopolymers, evidenced by decreased strengths over the same curing periods [48].

4.6. Drying Shrinkage

The variation in mortar shrinkage over time for different activators (NaOH, KOH, NaOH + Na_2SiO_3 , and KOH + Na_2SiO_3) is illustrated in Fig. (9). At a Water-to-Binder (W/B) ratio of 0.5, significant differences were observed after 3 days, with shrinkage values ranging from a minimum of 187.5 μm (M4E) to a maximum of 5237.5 μm (M9S) with a convergence of values between the other activators. We estimated the increase in shrinkage at 153% than the reference sample. The same trend was observed at 7 and 14 days. However, after 28 days, significant differences in shrinkage values were observed, with values ranging from 4331.25 μm to 4587.5 μm for M4S and M9E, and from 6918.7 μm to 8718.75 μm for M1E, M1S, M7E, and M9S. M7S recorded a maximum value of 10,875 μm , representing an increase of 224%.

The addition of silica fume to metakaolin-based geopolymer mortars reduced the drying shrinkage in MK geopolymer mortars by enhancing the matrix's density and reactivity. As a highly reactive material, silica fume contributes additional silicate content, promoting better geopolymerization and filling voids in the geopolymer matrix. Consequently, porosity decreases, and the capillary tension caused by water loss, both primary factors in drying shrinkage, is minimized [49].

Additionally, silica fume and solar curing may

significantly enhance shrinkage resistance. The heat from the sun-curing process activates the pozzolanic effects of silica fume, improving bonding within the geopolymer network and reducing the risk of shrinkage-induced cracks [50].

4.7. Bulk Density, Porosity, and Thermal Conductivity

Fig. (10) illustrates the compressive strength, bulk density, porosity, and thermal conductivity of mortar specimens, including OPC and geopolymer mortars with various binders (*e.g.*, silica fume, sodium silicate) and alkaline activators (NaOH, KOH), under ambient and solar curing conditions.

At a fixed w/b ratio, metakaolin geopolymer mortars demonstrate lower bulk density than OPC mortars, indicating increased porosity and enhanced thermal conductivity.

Silica fume mortars exhibit lower thermal conductivity (0.633-1.17 W/mK), primarily due to their higher porosity (20.65%-23.38%) and lower bulk density (1.92-1.97 g/cm^3). Under solar curing, thermal conductivity increases slightly due to reduced porosity and enhanced microstructural densification. In contrast, sodium silicate mortars have a higher thermal conductivity (1.19-1.68 W/mK), attributed to their lower porosity (13.09%-15.21%) and higher bulk density (2.01-2.09 g/cm^3). The incomplete geopolymerization in high Si/Al ratio samples (*e.g.*, 3.6) results in less dense geopolymer matrices [51]. Additionally, the porous structure significantly hinders heat transfer within the geopolymer network, effectively reducing its thermal conductivity (k) [52].

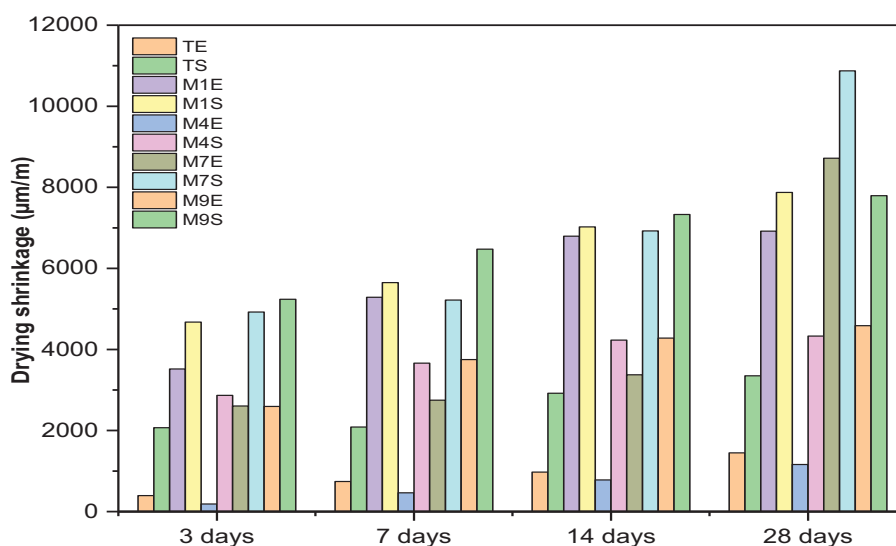


Fig. (9). Drying shrinkage of Geopolymer and OPC reference mortars at 3, 7, 14, and 28 days.

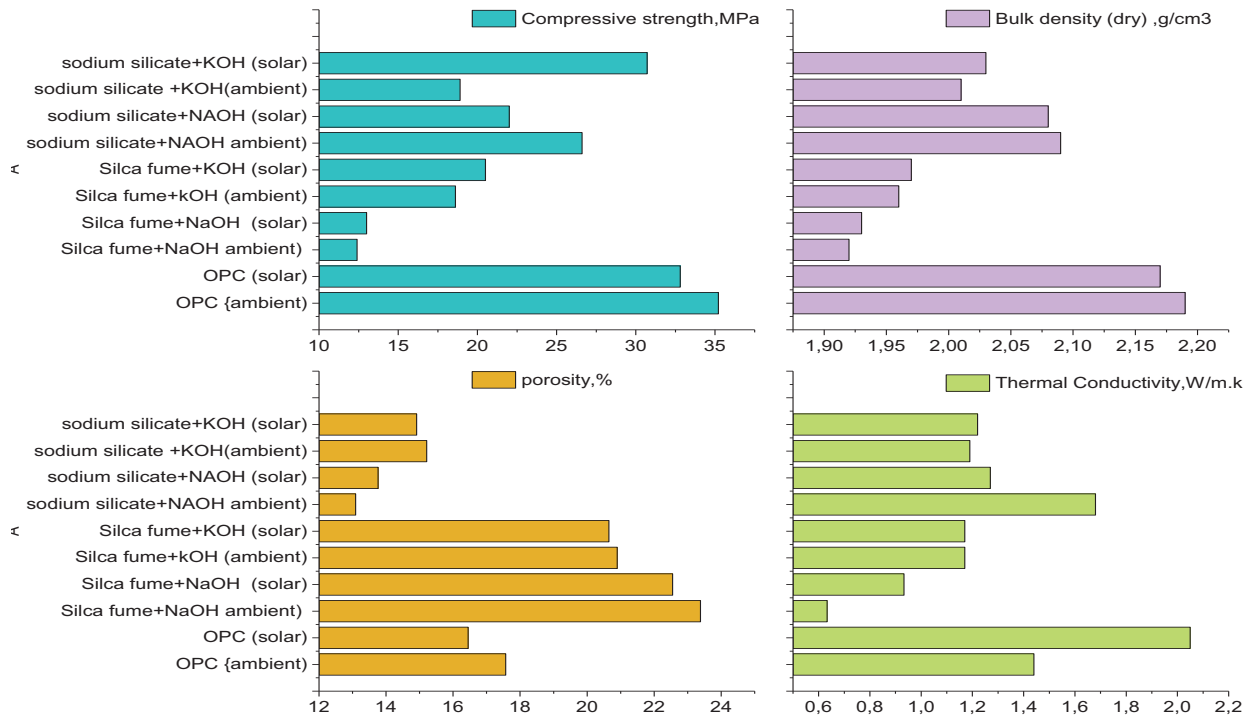


Fig. (10). Compressive strength, bulk density, porosity, and thermal conductivity of OPC and geopolymer mortars with W/b=0.5.

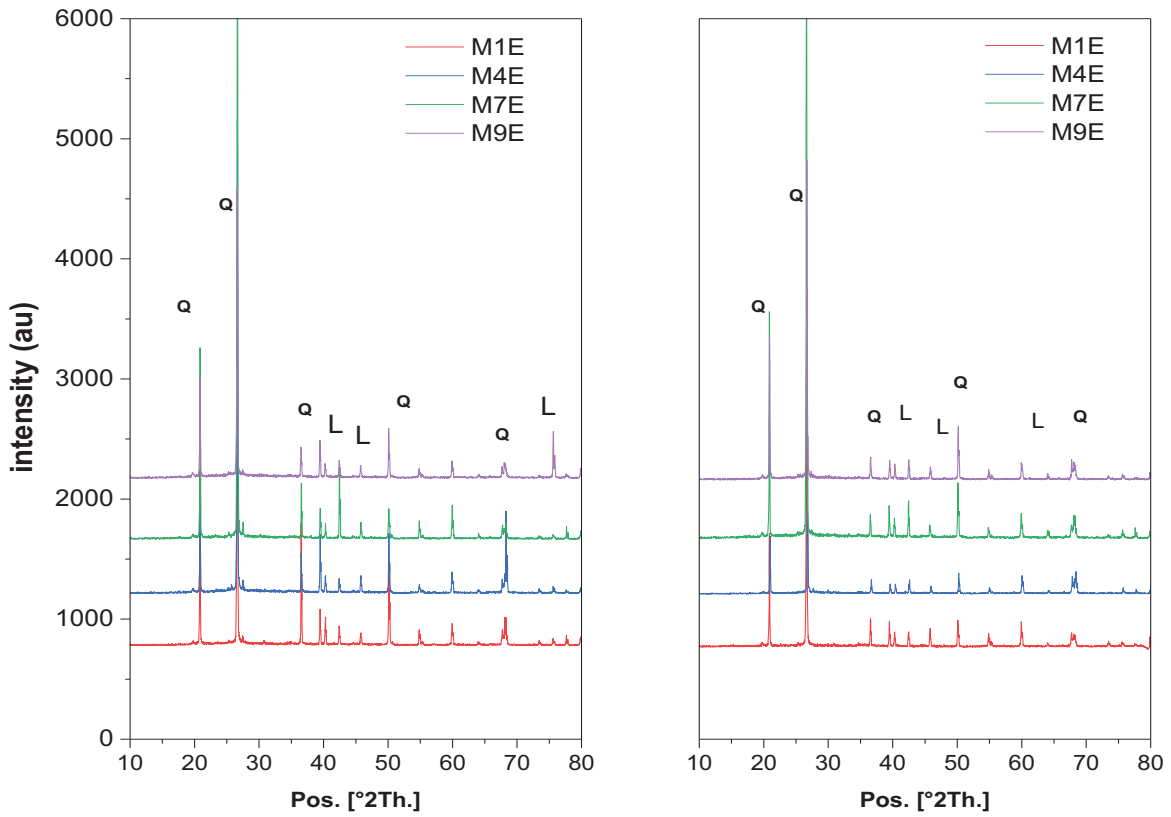


Fig. (11). XRD patterns of metakaolin geopolymer mortars: Q Quartz, L Leucite.

4.8. XRD Analysis of Metakaolin Geopolymer Mortars

In the conditions provided by the experiment, the formation of an amorphous geopolymer gel was expected due to the high silicon-to-aluminium (Si/Al) ratios (3.6 and 3.3), which promote the development of the amorphous gel while suppressing the growth of crystalline zeolite phases [53, 54]. The addition of silica fume increased the availability of reactive silica, which may lead to the stabilization of the amorphous gel and prevent secondary crystallization, including zeolite formation, even under high alkalinity conditions (13.389M and 19M), consistent with previous studies [55].

Based on X-ray diffraction analysis Fig. (11), Leucite (PDF: 01-076-2298) was observed in most sun-cured samples, likely due to pore closure and leucite formation as the microstructure evolves under elevated temperatures [56]. Quartz (PDF: 01-070-3755) was the dominant mineral in the samples, showing strong peaks at angles (20.8° and 26.6° in 2 θ), which overshadowed weaker signals associated with zeolite and the amorphous gel, consistent with the findings of Juengsuwattananon *et al.* [57].

5. DISCUSSION

Adding silica fume to geopolymer mortars strengthens the material by promoting the formation of dense structures. These results align with the findings of Nmiri *et al.* [58], who showed that using reactive silica increases compressive and flexural strength. Additionally, solar curing accelerates geopolymerization by increasing heat, which enhances strength and reduces porosity, as shown in the study by Rashad *et al.* [59].

Our study has demonstrated the effectiveness of using low-quality clay in geopolymer applications, further supported by existing research. Studies indicate that calcination of low-quality clays, even at moderate temperatures, can activate aluminosilicate reactivity. For example, low-quality kaolin mixed with alkali activators has shown promising compressive strength values and microstructural densification [60, 61]. Although high-quality clays, such as pure kaolinite, exhibit superior reactivity due to their higher aluminosilicate availability, their cost and limited availability make them less sustainable than low-quality alternatives. The use of high-quality kaolinite ensures consistent geopolymerization processes and improved mechanical performance, as highlighted by Mutlu [62].

In contrast, low-quality clays have demonstrated potential in achieving comparable mechanical strength with careful optimization of alkali content and curing conditions, as shown in studies on geopolymeric cement derived from calcined low-quality kaolin [63]. Furthermore, low-quality clays are more abundant and economically viable, making them ideal for sustainable large-scale geopolymer applications [64]. Low-cost aluminosilicate clays have demonstrated their ability to produce durable and environmentally friendly materials, strengthening the case for adopting low-quality clay as a viable and sustainable option in geopolymer production.

The comparison between low-quality and high-quality

clay demonstrates the feasibility of using local, low-quality resources for geopolymer production. These findings support that sustainable and cost-effective alternatives can be achieved with proper material processing and optimization.

Solar curing proved particularly effective in hot and arid climates, enhancing the mechanical and thermal performance of geopolymeric mortars. Similar to the findings by Işıklıdağ and Yalghuz [65], who demonstrated that elevated temperatures during heat curing significantly improved the strength and durability of metakaolin-based geopolymer mortars, solar curing leverages natural heat from sunlight to achieve comparable benefits, demonstrating its practicality for real-world applications in extreme climates.

The environmental impact of geopolymers extends beyond reducing carbon emissions compared to Portland cement to include additional benefits when evaluating their life cycle. Utilizing low-quality local materials or industrial by-products offers a sustainable alternative that reduces the environmental impacts associated with resource extraction and transportation [66]. Furthermore, calcining metakaolin or low-quality clays at moderate temperatures consumes significantly less energy compared to producing the clinker used in conventional cement [56]. Several studies [67, 68] demonstrated that energy consumption can be significantly reduced using sustainable curing techniques, such as solar curing. Additionally, the long lifespan and chemical stability of geopolymers reduce the need for frequent maintenance and replacement, thereby lowering long-term environmental impacts. Finally, the potential to recycle geopolymeric materials at the end of their life cycle enhances their role in a circular economy and minimizes waste directed to landfills.

CONCLUSION

This study examines the potential of local moderate kaolinitic clay as a suitable pozzolanic material, emphasizing its suitability for geopolymer mortar formulations. The properties of MK geopolymer mortars are significantly influenced by both the varieties of alkaline activators and the curing conditions. The present study yielded the following main conclusions:

- [1] Compressive and flexural strength values for geopolymer mortars differ according to the curing method and type of alkaline activator used.
- [2] In comparison, samples cured in the sun demonstrated a more than 40% increase in strength, most of which were better than Portland cement mortar.
- [3] Tests also indicate that KOH promotes better strength than NaOH, although NaOH initially facilitates more efficient dissolution and geopolymerization processes.
- [4] Higher strength is generated with lower H₂O/M₂O ratios, while higher values of the ratios result in increased porosity and lower strength.
- [5] Adding silica fume reduces drying shrinkage, and the thermal conductivity of geopolymer mortars depends on their structure and composition.
- [6] The geopolymer mortars are highly suitable for structures in hot-arid regions, offering great potential for energy-

efficient residential and infrastructure development due to their enhanced thermal properties and low shrinkage ratios. Their application extends to passive cooling systems, reducing dependence on energy-intensive climate control mechanisms.

- [7] Standardizing curing protocols and incorporating low-cost additives like agricultural residues will facilitate the economic viability and practical workability of geopolymer mortars for widespread adoption. Thorough studies on their long-term durability under real-world conditions are also crucial to prove their reliability, enabling broader adoption within the construction sector.

FUTURE WORK

This study is a preliminary independent work, *i.e.*, original experimental research on using a new binder based on local materials within a 3-phase timeframe: 3 days, 14 days, and 28 days, carried out in a region with an arid climate. It will be followed by another independent study focusing on the property of 'durability,' with the duration extended to 90, 180, and 365 days to assess the long-term durability of the mortar with this new binder.

AUTHORS' CONTRIBUTION

It is hereby acknowledged that all authors have accepted responsibility for the manuscript's content and consented to its submission. They have meticulously reviewed all results and unanimously approved the final version of the manuscript.

LIST OF ABBREVIATIONS

FS	=	Silica Fume.
KOH	=	Potassium Hydroxide
NaOH	=	Sodium Hydroxide
Na ₂ SO ₄	=	Sodium Silicate
K ₂ SiO ₃	=	Potassium Silicate
GPC	=	Geopolymer Concrete
OPC	=	Ordinary Portland Cement
FTIR	=	Fourier Transform Infrared
XRD	=	X-Ray Diffraction

CONSENT FOR PUBLICATION

Not applicable.

AVAILABILITY OF DATA AND MATERIALS

The data supporting the findings of this article is available within the manuscript.

FUNDING

None.

CONFLICT OF INTEREST

The authors declare no conflict of interest, financial or otherwise

ACKNOWLEDGEMENTS

The author would like to thank the staff of STG's Adrar cement plant and the engineers of the laboratory of the university Ahmed Draya Adrar, for their contributions.

REFERENCES

- [1] Y. Zhang, A. Tariq, A.C. Hughes, D. Hong, F. Wei, H. Sun, J. Sardans, J. Peñuelas, G. Perry, J. Qiao, A. Kurban, X. Jia, D. Raimondo, B. Pan, W. Yang, D. Zhang, W. Li, Z. Ahmed, C. Beierkuhnlein, G. Lazkov, K. Toderich, S. Karryeva, D. Dehkonov, H. Hisoriev, L. Dimeyeva, D. Milko, A. Soule, M. Suska-Malawska, J. Saparmuradov, A. Bekzod, P. Allin, S. Dieye, B. Cisse, W. Whibesilassie, and K. Ma, "Challenges and solutions to biodiversity conservation in arid lands", *Sci. Total Environ.*, vol. 857, no. Pt 3, p. 159695, 2023. [<http://dx.doi.org/10.1016/j.scitotenv.2022.159695>] [PMID: 36302433]
- [2] T.J. Lawrence, J.M. Vilbig, G. Kangogo, E.M. Fèvre, S.L. Deem, I. Gluecks, V. Sagan, and E. Shacham, "Shifting climate zones and expanding tropical and arid climate regions across Kenya (1980-2020)", *Reg. Environ. Change*, vol. 23, no. 2, p. 59, 2023. [<http://dx.doi.org/10.1007/s10113-023-02055-w>]
- [3] M.R. Houmsi, M.S. Shiru, M.S. Nashwan, K. Ahmed, G.F. Ziarh, S. Shahid, E-S. Chung, S. Kim, and S. Kim, "Spatial shift of aridity and its impact on land use of syria", *Sustainability (Basel)*, vol. 11, no. 24, p. 7047, 2019. [<http://dx.doi.org/10.3390/su11247047>]
- [4] A. Abulibdeh, "Planning for congestion pricing policies in the middle east: Public acceptability and revenue distribution", *Transp. Lett.*, vol. 14, no. 3, pp. 282-297, 2022. [<http://dx.doi.org/10.1080/19427867.2020.1857908>]
- [5] A. Abulibdeh, "Analysis of urban heat island characteristics and mitigation strategies for eight arid and semi-arid gulf region cities", *Environ. Earth Sci.*, vol. 80, no. 7, p. 259, 2021. [<http://dx.doi.org/10.1007/s12665-021-09540-7>] [PMID: 33777247]
- [6] P. Cerutti, "Urban heat islands, global heating, heat exchange, ground source heat pumps", *Ital. J. Ground.*, vol. 12, no. 1, p. 738, 2023. [<http://dx.doi.org/10.7343/as-2023-738>]
- [7] M. Schneider, "The cement industry on the way to a low-carbon future", *Cement Concr. Res.*, vol. 124, p. 105792, 2019. [<http://dx.doi.org/10.1016/j.cemconres.2019.105792>]
- [8] B.B. Jindal, "Feasibility study of ambient cured geopolymer concrete-A review", *Advances in Concrete Construction*, vol. 6, no. 4, p. 387, 2018. [<http://dx.doi.org/10.12989/acc.2018.6.4.387>]
- [9] S. Sultana, "Chapter 4 - Urban heat island: Land cover changes, management, and mitigation strategies", In: *Global Urban Heat Island Mitigation*, Elsevier: Amsterdam, Netherlands, 2022, pp. 71-93. [<http://dx.doi.org/10.1016/B978-0-323-85539-6.00009-3>]
- [10] A. Odeh, A. Al-Fakih, M. Alghannam, M. Al-Ainya, H. Khalid, M.A. Al-Shugaa, B.S. Thomas, and M. Aswin, "Recent progress in geopolymer concrete technology: A review", *Civ. Eng. (Shiraz)*, vol. 48, no. 5, pp. 3285-3308, 2024. [<http://dx.doi.org/10.1007/s40996-024-01391-z>]
- [11] M. Nanthini, R. Ganesan, and V. Jaganathan, "Studies on alkaline activator, manufacturing methods and mechanical properties of geopolymer concrete - a review", *J. Environ. Nanotechnol.*, vol. 13, no. 3, pp. 52-72, 2024. [<http://dx.doi.org/10.13074/jent.2024.09.242753>]
- [12] Z. Ji, L. Su, and Y. Pei, "Characterization and adsorption performance of waste-based porous open-cell geopolymer with one-pot preparation", *Ceram. Int.*, vol. 47, no. 9, pp. 12153-12162, 2021. [<http://dx.doi.org/10.1016/j.ceramint.2021.01.062>]
- [13] A. Bassoud, H. Khelafi, A.M. Mokhtari, and A. Bada, "Evaluation of

- summer thermal comfort in arid desert areas. Case study: Old adobe building in Adrar (South of Algeria)", *Build. Environ.*, vol. 205, p. 108140, 2021.
[<http://dx.doi.org/10.1016/j.buildenv.2021.108140>]
- [14] R. Farhan Ramadan, H. Ghanem, J. Khatib, and A. Elkordi, "Effect of hot weather concrete on the mechanical and durability properties of concrete - a review", *BAU J. - Sci. Technol.*, vol. 4, no. 1, 2022.
[<http://dx.doi.org/10.54729/AXEC5733>]
- [15] M. Rabie, M.R. Irshidat, and N. Al-Nuaimi, "Ambient and heat-cured geopolymer composites: Mix design optimization and life cycle assessment", *Sustainability (Basel)*, vol. 14, no. 9, p. 4942, 2022.
[<http://dx.doi.org/10.3390/su14094942>]
- [16] G. M. Zannerni, K.P. Fattah, and A.K. Al-Tamimi, "Ambient-cured geopolymer concrete with single alkali activator", *Sustai. Mater. Technol.*, vol. 23, p. e00131, 2020.
[<http://dx.doi.org/10.1016/j.susmat.2019.e00131>]
- [17] R.P. Singh, and B. Mohanty, "Effect of slag on mechanical and microstructural properties of fly ash-based geopolymer concrete containing recycled aggregate", *J. Phys.: Conf. Ser.*, vol. 2779, p. 012017, 2024.
[<http://dx.doi.org/10.1088/1742-6596/2779/1/012017>]
- [18] B.B.J.A.i.c.c. Jindal, "Feasibility study of ambient cured geopolymer concrete", *A review.*, vol. 6, no. 4, p. 387, 2018.
[<http://dx.doi.org/10.12989/acc.2018.6.4.387>]
- [19] T. Alomayri, "Experimental study of the microstructural and mechanical properties of geopolymer paste with nano material (Al₂O₃)", *J. Build. Eng.*, vol. 25, p. 100788, 2019.
[<http://dx.doi.org/10.1016/j.jobe.2019.100788>]
- [20] M. Abd Ellatief, A.A. Abadel, K. Federowicz, and M. Abd Elrahman, "Mechanical properties, high temperature resistance and microstructure of eco-friendly ultra-high performance geopolymer concrete: Role of ceramic waste addition", *Constr. Build. Mater.*, vol. 401, p. 132677, 2023.
[<http://dx.doi.org/10.1016/j.conbuildmat.2023.132677>]
- [21] W. Hu, Q. Nie, B. Huang, and X. Shu, "Investigation of the strength development of cast-in-place geopolymer piles with heating systems", *J. Clean. Prod.*, vol. 215, pp. 1481-1489, 2019.
[<http://dx.doi.org/10.1016/j.jclepro.2019.01.155>]
- [22] A. Alaskar, M.S. Mahmood, R.U.D. Nassar, O. Zaid, F. Althoey, and M.M. Arbili, "Systematic review on geopolymer composites modified with nanomaterials and thin films: Enhancing performance and sustainability in construction", *Constr. Build. Mater.*, vol. 409, p. 133888, 2023.
[<http://dx.doi.org/10.1016/j.conbuildmat.2023.133888>]
- [23] X. Wu, Y. Shen, and L. Hu, "Performance of geopolymer concrete activated by sodium silicate and silica fume activator", *Case Stud. Construc. Mater.*, vol. 17, p. e01513, 2022.
[<http://dx.doi.org/10.1016/j.cscm.2022.e01513>]
- [24] M. Mansourghanaei, M. Biklaryan, and A. Mardookhpour, "Experimental study of the effects of adding silica nanoparticles on the durability of geopolymer concrete", *Aust. J. Civ. Eng.*, vol. 22, no. 1, pp. 81-93, 2024.
[<http://dx.doi.org/10.1080/14488353.2022.2120247>]
- [25] O. Youssf, M. Elchalakani, R. Hassanli, R. Roychand, Y. Zhuge, R.J. Gravina, and J.E. Mills, "Mechanical performance and durability of geopolymer lightweight rubber concrete", *J. Build. Eng.*, vol. 45, p. 103608, 2022.
[<http://dx.doi.org/10.1016/j.jobe.2021.103608>]
- [26] O.A. Mohamed, O. Najm, H.A. Zuaiter, S.K. Saleem, S. Ivak, and K. Al-Arife, "Effect of activator concentration on setting time, workability and compressive strength of sustainable concrete with alkali-activated slag binder", *Mater. Today Proc.*, vol. 4, p. 103, 2024.
[<http://dx.doi.org/10.1016/j.matpr.2024.04.103>]
- [27] D.G. Sayed, S.M.A. El-Gamal, F.I. El-Hosiny, M.M. Hazem, and M. Ramadan, "Promoting the performance of green slag-based geopolymer using eskolaite nanoparticles for bio-mechanical, thermal, and shielding applications", *Constr. Build. Mater.*, vol. 433, p. 136706, 2024.
[<http://dx.doi.org/10.1016/j.conbuildmat.2024.136706>]
- [28] M. El Dandachy, L. Hassoun, A. El-Mir, and J.M. Khatib, "Effect of elevated temperatures on compressive strength, ultrasonic pulse velocity, and transfer properties of metakaolin-based geopolymer mortars", *Buildings*, vol. 14, no. 7, p. 2126, 2024.
[<http://dx.doi.org/10.3390/buildings14072126>]
- [29] M.M. Ahmed, D. Tarek, and H.S. Hussein, "Building envelope optimization using geopolymer bricks to improve energy efficiency in residential buildings in hot-arid regions", *Case Stud. Construc. Mater.*, vol. 17, p. e01657, 2022.
[<http://dx.doi.org/10.1016/j.cscm.2022.e01657>]
- [30] Z. Emdadi, N. Asim, M. Ambar Yarmo, R. Shamsudin, M. Mohammad, and K. Sopian, "Green material prospects for passive evaporative cooling systems: Geopolymers", *Energies*, vol. 9, no. 8, p. 586, 2016.
[<http://dx.doi.org/10.3390/en9080586>]
- [31] H.M. Khater, and H.A. Abd el Gawaad, "Characterization of alkali activated geopolymer mortar doped with MWCNT", *Constr. Build. Mater.*, vol. 102, pp. 329-337, 2016.
[<http://dx.doi.org/10.1016/j.conbuildmat.2015.10.121>]
- [32] "Standard Test Methods for Sampling and Testing Fly Ash or Natural Pozzolans for Use in Portland-Cement Concrete", *ASTM Int.*, vol. 22, p. 311, 2024.
[http://dx.doi.org/10.1520/C0311_C0311M-22]
- [33] S. Mu, J. Liu, J. Liu, Y. Wang, L. Shi, and Q. Jiang, "Property and microstructure of waterborne self-setting geopolymer coating: Optimization effect of SiO₂/Na₂O molar ratio", *Minerals.*, vol. 8, no. 4, p. 162, 2018.
[<http://dx.doi.org/10.3390/min8040162>]
- [34] "DIN EN 196-1:2016-11. Methods of testing cement - Part 1: Determination of strength; German", *DIN EN Int.*, vol. 11, p. 416, 2016.
[<http://dx.doi.org/10.31030/2482416>]
- [35] "NF P15-433. Hydraulic binders - Methods of testing cement - Determination of shrinkage and swelling", *NF Int.*, vol. 15, pp. 429-433, 2023.
- [36] "ASTM C642-21. Standard Test Method for Density, Absorption, and Voids in Hardened Concrete", *ASTM Int.*, vol. 22, p. 0311, 2022.
[http://dx.doi.org/10.1520/C0311_C0311M-22]
- [37] G.G.O. Rodrigues, A.B. Rohden, V.R. Wiggers, and M.R. Garcez, "Reactivity of flash-calcined illitic clays", *Constr. Build. Mater.*, vol. 411, p. 134578, 2024.
[<http://dx.doi.org/10.1016/j.conbuildmat.2023.134578>]
- [38] R. Gobinath, P. Awoyera, N. Praveen, V. Babu, P. Sai, and K.J. Prathibha, "Effects of calcined clay on the engineering properties of cementitious mortars", *Mater. Tod.*, vol. 39, pp. 110-113, 2021.
[<http://dx.doi.org/10.1016/j.matpr.2020.06.322>]
- [39] "ASTM C618-17 Standard Specification for Coal Fly Ash and Raw or Calcined Natural Pozzolan for Use in Concrete", *ASTM Int.*, vol. 17, p. 618, 2017.
[http://dx.doi.org/10.1520/C0618_C0618M-17]
- [40] N. Tebbal, and Z.E.A.J.P.C.S. Rahmouni, "Rheological and mechanical behavior of mortars with metakaolin formulation",
[<http://dx.doi.org/10.1016/j.procs.2019.09.026>]
- [41] N.S. Msinjili, J.G. Gregor, P. Gluth, S.N. Vogler, and H.-C. Kühne, "Comparison of calcined illitic clays (brick clays) and low-grade kaolinitic clays as supplementary cementitious materials", *Mater. Struct.*, vol. 52, no. 94, p. 1393, 2019.
[<http://dx.doi.org/10.1617/s11527-019-1393-2>]
- [42] G. Liang, W. Yao, and A. She, "New insights into the early-age reaction kinetics of metakaolin geopolymer by 1H low-field NMR and isothermal calorimetry", *Cement Concr. Compos.*, vol. 137, p. 104932, 2023.
[<http://dx.doi.org/10.1016/j.cemconcomp.2023.104932>]
- [43] X. Zhu, H. Qian, H. Wu, Q. Zhou, H. Feng, Q. Zeng, Y. Tian, S. Ruan, Y. Zhang, S. Chen, and D. Yan, "Early-stage geopolymerization process of metakaolin-based geopolymer", *Materials (Basel)*, vol. 15, no. 17, p. 6125, 2022.

- [http://dx.doi.org/10.3390/ma15176125] [PMID: 36079507]
- [44] R.O.A. Alftah, S.A.A. Elbaky, G. Ghanem, and D.M. Sadek, "Effect of exposure to elevated temperatures on geopolymer concrete properties", *Al-Azhar Univer. Civ. Enginee. Res. Mag.*, vol. 10, no. 10, pp. 448-461, 2019.
- [45] D.P. Dias, and F. de Andrade Silva, "Effect of Na₂O/SiO₂ and K₂O/SiO₂ mass ratios on the compressive strength of non-silicate metakaolin geopolymeric mortars", *Mater. Res. Exp.*, vol. 6, no. 7, p. 179, 2019.
[http://dx.doi.org/10.1088/2053-1591/ab179d]
- [46] D.M. González-García, L. Téllez-Jurado, F.J. Jiménez-Álvarez, L. Zarazua-Villalobos, and H. Balmori-Ramírez, "Evolution of a natural pozzolan-based geopolymer alkalinized in the presence of sodium or potassium silicate/hydroxide solution", *Constr. Build. Mater.*, vol. 321, p. 126305, 2022.
[http://dx.doi.org/10.1016/j.conbuildmat.2021.126305]
- [47] M. Amer Salih, N. Farzadnia, R. Demirboga, and A.A.A. Ali, "Effect of elevated temperatures on mechanical and microstructural properties of alkali-activated mortar made up of POFA and GGBS", *Constr. Build. Mater.*, vol. 328, p. 127041, 2022.
[http://dx.doi.org/10.1016/j.conbuildmat.2022.127041]
- [48] M. Muracchioli, G. Menardi, M. D' Agostini, G. Franchin, and P. Colombo, "Modeling the compressive strength of metakaolin-based geopolymers based on the statistical analysis of experimental data", *Appl. Clay Sci.*, vol. 242, p. 107020, 2023.
[http://dx.doi.org/10.1016/j.clay.2023.107020]
- [49] G. Sadeghian, K. Behfarnia, and M. Teymouri, "Drying shrinkage of one-part alkali-activated slag concrete", *J. Build. Eng.*, vol. 51, p. 104263, 2022.
[http://dx.doi.org/10.1016/j.jobe.2022.104263]
- [50] D. Xu, J. Tang, X. Hu, Y. Zhou, C. Yu, F. Han, and J. Liu, "Influence of silica fume and thermal curing on long-term hydration, microstructure and compressive strength of ultra-high performance concrete (UHPC)", *Constr. Build. Mater.*, vol. 395, p. 132370, 2023.
[http://dx.doi.org/10.1016/j.conbuildmat.2023.132370]
- [51] Y. Liu, C. Lu, X. Hu, and C. Shi, "Effect of silica fume on rheology of slag-fly ash-silica fume-based geopolymer pastes with different activators", *Cement Concr. Res.*, vol. 174, p. 107336, 2023.
[http://dx.doi.org/10.1016/j.cemconres.2023.107336]
- [52] Y. Luo, C.H. Koh, S.H. Li, H.J.H. Brouwers, and Q. Yu, "Understanding the thermal behavior of geopolymeric composites designed by packing model", *Cement Concr. Compos.*, vol. 143, p. 105265, 2023.
[http://dx.doi.org/10.1016/j.cemconcomp.2023.105265]
- [53] H.M. Khater, "Effect of silica fume on the characterization of the geopolymer materials", *Int. J. Adv. Struc. Enginee.*, vol. 5, no. 1, p. 12, 2013.
[http://dx.doi.org/10.1186/2008-6695-5-12]
- [54] F. Oshani, A. Allahverdi, A. Kargari, R. Norouzbeigi, and N.M. Mahmoodi, "Effect of preparation parameters on properties of metakaolin-based geopolymer activated by silica fume-sodium hydroxide alkaline blend", *J. Build. Enginee.*, vol. 60, p. 104984, 2022.
[http://dx.doi.org/10.1016/j.jobe.2022.104984]
- [55] Q. Wan, F. Rao, S. Song, R.E. García, R.M. Estrella, C.L. Patiño, and Y. Zhang, "Geopolymerization reaction, microstructure and simulation of metakaolin-based geopolymers at extended Si/Al ratios", *Ceme. Concr. Comp.*, vol. 79, pp. 45-52, 2017.
[http://dx.doi.org/10.1016/j.cemconcomp.2017.01.014]
- [56] Y. Lu, N. Cui, Y. Xian, J. Liu, C. Xing, N. Xie, and D. Wang, "Microstructure evolution mechanism of geopolymers with exposure to high-temperature environment", *Crystals (Basel)*, vol. 11, no. 9, p. 1062, 2021.
[http://dx.doi.org/10.3390/cryst11091062]
- [57] K. Juengsuwattananon, F. Winnefeld, P. Chindaprasirt, and K. Pimraksa, "Correlation between initial SiO₂/Al₂O₃, Na₂O/Al₂O₃, Na₂O/SiO₂ and H₂O/Na₂O ratios on phase and microstructure of reaction products of metakaolin-rice husk ash geopolymer", *Constr. Build. Mater.*, vol. 226, pp. 406-417, 2019.
[http://dx.doi.org/10.1016/j.conbuildmat.2019.07.146]
- [58] A. Nmiri, L.Y. Ming, H.C. Yong, and M.F.M. Tahir, "Temperature effect on mechanical and physical properties of Na or K alkaline silicate activated metakaolin-based geopolymers", *Cement Based Materials*, Intechopen: London, UK, p. 74438, 2016.
[http://dx.doi.org/10.5772/intechopen.74438]
- [59] A.M. Rashad, Y.A. Mosleh, and M.M. Mokhtar, "Thermal insulation and durability of alkali-activated lightweight slag mortar modified with silica fume and fly ash", *Constr. Build. Mater.*, vol. 411, p. 134255, 2024.
[http://dx.doi.org/10.1016/j.conbuildmat.2023.134255]
- [60] M.X. Peng, Z.H. Wang, and S.H. Shen, "Synthesis, characterization and mechanisms of one-part geopolymeric cement by calcining low-quality kaolin with alkali", *Mater. Struct.*, vol. 48, pp. 699-708, 2015.
[http://dx.doi.org/10.1617/s11527-014-0350-3]
- [61] Z.H. Zhang, H.J. Zhu, C.H. Zhou, and H. Wang, "Geopolymer from kaolin in China: An overview", *Appl. Clay Sci.*, vol. 119, pp. 31-41, 2016.
[http://dx.doi.org/10.1016/j.clay.2015.04.023]
- [62] H.K. Mutlu, "High-strength tile production from yellow clay with high silicon dioxide content and its reflection in ultraviolet and visible regions", *Case Stud. Construc. Mater.*, vol. 21, p. e03534, 2024.
[http://dx.doi.org/10.1016/j.cscm.2024.e03534]
- [63] T.T. Lan, N.A. Duong, P.L. Anh, and T.T. Man, "Research on fabrication of non-calcined geopolymer ceramics from kaolin Tung Ba, Vi Xuyen", *Ha Giang.*, vol. 41, no. 4, pp. 388-402, 2019.
[http://dx.doi.org/10.15625/0866-7187/41/4/14371]
- [64] I. Labaied, O. Douzane, G. Promis, and M. Lajili, "Synthesis of alkali-activated materials blended with fly ash: Optimization of curing conditions and precursor dosage", *J. Build. Enginee.*, vol. 79, p. 107863, 2023.
[http://dx.doi.org/10.1016/j.jobe.2023.107863]
- [65] B. Işıkdağ, and M.R. Yalghuz, "Strength development and durability of metakaolin geopolymer mortars containing pozzolans under different curing conditions", *Minerals.*, vol. 13, no. 7, p. 857, 2023.
[http://dx.doi.org/10.3390/min13070857]
- [66] M.S. Saif, M.O.R. El-Hariri, A.I. Sarie-Eldin, B.A. Tayeh, and M.F. Farag, "Impact of Ca+ content and curing condition on durability performance of metakaolin-based geopolymer mortars", *Case Stud. Construc. Mater.*, vol. 16, p. e00922, 2022.
[http://dx.doi.org/10.1016/j.cscm.2022.e00922]
- [67] S.A. Khan, A. Kul, O. Şahin, M. Şahmaran, S.G. Al-Ghamdi, and M. Koç, "Energy-environmental performance assessment and cleaner energy solutions for a novel Construction and Demolition Waste-based geopolymer binder production process", *Ener. Rep.*, vol. 8, pp. 14464-14475, 2022.
[http://dx.doi.org/10.1016/j.egy.2022.10.345]
- [68] J. Zhao, L. Tong, B. Li, T. Chen, C. Wang, G. Yang, and Y. Zheng, "Eco-friendly geopolymer materials: A review of performance improvement, potential application and sustainability assessment", *J. Clean. Produc.*, vol. 307, p. 127085, 2021.
[http://dx.doi.org/10.1016/j.jclepro.2021.127085]